

# Canon: Exploiting Channel Diversity for Reliable Parallel Decoding in Backscatter Communication

Chengkun Jiang, Yuan He, Meng Jin, Xiaolong Zheng, Junchen Guo

School of Software and BNRist, Tsinghua University

{jck15, gjc16}@mails.tsinghua.edu.cn, {heyuan, mengj, zhengxiaolong}@mail.tsinghua.edu.cn

**Abstract**—Backscatter communication, due to its low energy consumption, attract a broad range of applications. The throughput of such low-power communication is however limited. Parallel backscatter is deemed as a promising technique for improving the overall throughput by enabling concurrent transmissions of the backscattering tags. The state-of-the-art approaches for parallel backscatter assume that all the states of the collided signals are distinguishable in the In-phase and Quadrature (IQ) signal plane. In this paper, we disclose the superclustering phenomenon that makes the assumption untenable and significantly degrades the overall performance. Moreover, we observe that the indistinguishable states at different channels are not the same due to the intrinsic channel diversity. Motivated by the observation, we propose Canon, an approach that exploits the channel diversity of the backscatter tags for reliable parallel decoding. In Canon, we address two critical challenges: (i) designing the Multi-Carrier Backscatter (MCB) module to extract the collided signals simultaneously from multiple channels, (ii) designing the Multi-Channel Cluster Union (MCCU) algorithm to distinguish each state of the collided signals. The experiments demonstrate that Canon can achieve over  $10\times$  higher throughput than the state-of-the-art approaches.

**Index Terms**—Backscatter; Parallel Decoding; Multiple Channels; Concurrent Transmission

## I. INTRODUCTION

Backscatter communication, due to its low energy consumption, becomes a promising solution in many applications such as warehouse inventory and retailing [1]–[4]. In such applications, large volumes of data generated by the densely-deployed tags need be transmitted and processed. How to effectively collect those data becomes a crucial problem. Parallel backscatter is therefore proposed to improve the overall throughput by enabling the concurrent transmissions of the tags.

Researchers have proposed many approaches for parallel decoding of multiple tags [5]–[12]. In a typical backscatter system, the tags modulate their data by reflecting or absorbing the excitation signals from the sender, which results in two different states correspondingly. The receiver decodes the data based on the transition between the two states. As for parallel backscatter, the collided signals from multiple tags will generate more different states and it is important to distinguish all the states before the decoding. The existing approaches like BiGroup [6] and FlipTracer [7] exploit the features from the time domain and the IQ domain to distinguish all the states for the tags and then decode the tags' data based on the transitions among the states. A key assumption behind those works is

that one can distinguish all the different states of the collided signals. However, in our real-world experiments, we find the assumption is untenable due to the so-called superclustering phenomenon.

The samples of the same states of the collided signals actually spread within a cluster in the IQ plane rather than fall onto one point theoretically. The size of the cluster is generally determined by the noise level. Therefore, the collided signals may form different clusters in the IQ plane. Superclustering refers to the following phenomenon: those clusters overlap with each other so that it is unable to clearly separate every cluster. There are two main reasons for the superclustering phenomenon that invalidates the aforementioned assumption. First, the Signal-to-Noise-Ratio (SNR) is relatively low at the receiver. Generally, the noise level determines the size of the cluster and the signal strength determines the inter-cluster distance. The relatively low SNR of the tag will lead to the larger cluster size and shorter inter-cluster distance. When the clusters are close to each other, they are likely to overlap with each other and the supercluster appears.

Second, the number of the clusters increases exponentially with the number of the concurrently-transmitting tags. For  $N$  tags, there are  $2^N$  clusters in the IQ plane. Therefore, when the collided signals are formed by a large number of tags, the limited space in the IQ plane and the large number of the clusters inevitably result in the severe superclustering. Existing approaches are unreliable and error-prone to distinguish all the states of the collided signals, with the existence of superclusters.

In order to address the above challenges, we in this paper propose Canon, an approach that can reliably decode the collided signals of the concurrently-transmitting tags in practical scenarios. We observe that the tag's IQ signals are different when the excitation signals are sent at different channels. A backscatter tag can actually transmit the signal within a large frequency band simultaneously. In other words, if we can transmit the excitation signals at multiple channels, we can extract the tag's signals at every channel. The channel diversity and the transmission at multiple channels increase the opportunity for reliably decoding the tags' collided signals. If we can obtain the collided IQ signals at multiple channels, the superclusters at each channel will be different because of the channel diversity. Then we can exploit the IQ clusters from all the channels to find the correct  $2^N$  representations for each state of the collided tags.

In Canon, we design the Multi-Carrier Backscatter (MCB) module to enable the multi-channel transmissions of the backscatter signals and design the Multi-Channel Cluster Union (MCCU) algorithm that exploits the channel diversity to reliably decode the tags' data concurrently. The main contributions of Canon are as follows:

- We observe the superclustering phenomenon of parallel backscatter in practice. The superclusters may widely exist because of the tag's weak signal and the sensitivity to the channel noise. Furthermore, increase in the number of tags may also aggravate superclustering. This phenomenon severely affect the performance of the state-of-the-art IQ-based parallel decoding approaches.
- In Canon, we design the MCB module to enable the tag's transmissions at multiple channels and propose the MCCU algorithm to reliably decode the tags' data with the multi-channel IQ signals.
- We implement a practical system to evaluate Canon. The experiment results demonstrate that Canon can reliably decode the collided signals and achieve 10× higher throughput than the state-of-the-art approach.

In the rest of the paper, we discuss related works in Section II, and describe the motivation of our design in Section III. The design details of Canon are presented in Sections IV, V, VI and VII. Section VIII evaluates the performance of Canon. We conclude the paper in Section IX.

## II. RELATED WORKS

Many efforts have been made to improve the throughput of backscatter communication from many directions. We classify them into the following two categories:

**Supporting parallel transmission.** Parallel transmission has the potential for multiplexing the throughput of backscatter communication. Early methods for parallel transmission is to exploit coding mechanisms [10], [11], [13]–[15] on tags to facilitate collision recovery. The main idea of these works is to exploit an orthogonal code for encoding data, where the tags have to convert each bit to a long PN sequence (hundreds of bits in length). CDMA based methods are however inefficient for backscatter communication because tags have to toggle the transmit antenna more frequently, which increases power consumption by orders of magnitude [5], [9].

To solve this problem, some recent works propose to decode concurrent transmissions by extending the decoding capacity at the reader side. [5]–[7], [12], [16]–[18]. In these works, the reader decodes the collided signal according to the signals' features at time and/or IQ domain. For example, [5], [9], [12] propose that the reader can identify the collided signals based on their IQ domain positions. BiGroup [6] and LF-backscatter [9] assume that the signal edges of the same tag will come at a relatively fixed interval (i.e., stable bit duration). Thus they can separate the signal edges of different tags in the time domain, and connect with the signal clusters in the IQ domain for collision decoding. FlipTracer [7] identifies the collided signal using signal's transition probability between different signal clusters.

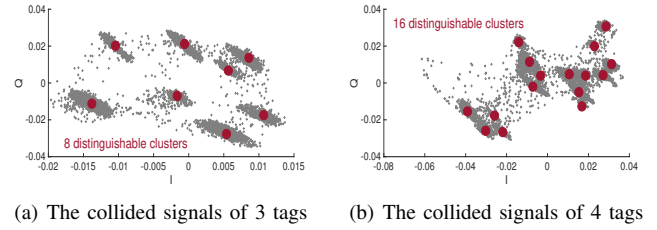


Fig. 1. The distribution of the IQ symbols for the collided signals

Although the above methods enable parallel transmissions without introducing additional complexity at the tag, our study reveals that the main problem of these method is they can't work at practical scenarios. The main reason is that they require all the signal clusters of the collided signal are separated at IQ domain. This assumption is however unrealistic in practical backscatter systems. Specifically, in backscatter systems, the SNR of the backscatter signal decays significantly with the transmission distance and the number of signal clusters (which represent the combined states) increases exponentially with the number of tags, which both incur seriously superclustering phenomenon and lead to low decoding rate. Canon is therefore proposed to solve this problem by exploiting channel diversity.

**Exploiting channel diversity in backscatter networks.** Some works propose to improve the throughput by exploiting channel diversity in backscatter network [19]–[21]. Specifically, they claim that: for a specific tag, the channel quality varies among different channels; for a specific channel, different tags have diverse channel qualities. These works exploit these characteristics to enable more accurate channel selection and rate adaptation, and therefore improve the throughput. Different from these works, Canon exploits channel diversity for more reliable parallel transmission of tags, which yields significant throughput improvement compared with the above serial transmission works.

Although some FDMA based works have been proposed to enable parallel transmission, they are inefficient for backscatter communication [22]–[24]. The main reasons are that: i) they require a strict symbol level synchronization among the transmissions, which is unrealistic for the low cost backscatter tags. ii) they require that different tags transmit at orthogonal subcarriers, while creating frequency shift is a tough task for backscatter tags. Different from the above methods, Canon exploits channel diversity for parallel transmission without requiring any modification or incurring any additional overhead on the tags.

## III. PRELIMINARY STUDY

### A. The Superclustering of the Collided Signals

The tag's data is encoded by the reflection and the absorption of the excitation signal, which will result in two states of the received signal, denoted as High (H) and Low (L) states. When there are  $N$  tags concurrently transmitting, the collided signals will have  $2^N$  distinct combined states. For example, there are 4 combined states (HH, HL, LH, LL) for 2 tags. The

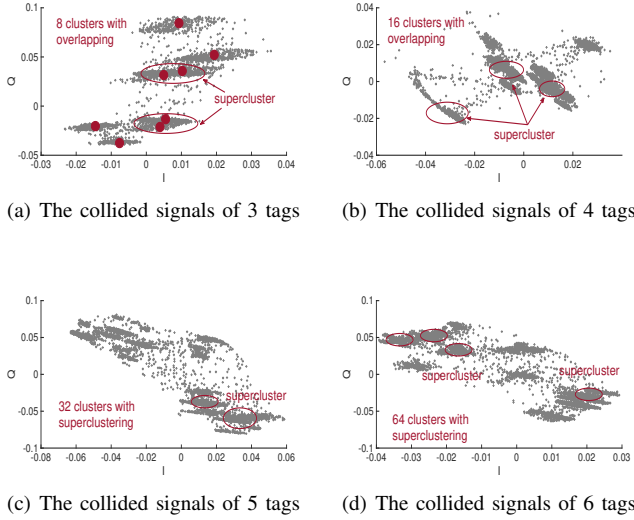


Fig. 2. The distribution of the IQ symbols for the collided signals when the SNRs are low

state-of-the-art approaches propose to use the IQ features to distinguish the  $2^N$  combined states since  $N$  tags will result in  $2^N$  IQ symbol clusters in the IQ plane. Fig. 1 presents the distributions of the IQ symbols when there are 3 and 4 tags transmitting concurrently. It can be obviously observed that they form 8 and 16 clusters respectively.

In practical environments, however, the clusters are not always distinguishable as shown in Fig. 1. Backscatter tags have low SNRs and can be easily affected by the background noise or other interference at the same frequency band. The size of the cluster can be decided by the channel noise and the inter-cluster distance indicates the signal strength of the tag. Therefore, the distances between these clusters can be very close and the halos of these clusters can be very large, which can lead to the IQ symbol distributions as shown in Fig. 2. The clustering algorithm used in previous works will fail to find correct 8 and 16 clusters in such scenarios. We refer the phenomenon as superclustering.

The superclustering will also happen when the number of the tags is large because the number of the clusters will increase exponentially with the number of the tags. Fig. 2(c) and 2(d) show the IQ planes in such scenarios with 5 and 6 tags. Existing approaches will fail to decode the tags when they can't find the correct  $2^N$  clusters in the IQ plane. It is challenging to decode the collided signal reliably because somehow we will meet the superclustering caused by either the low SNR or large number of the tags and the  $2^N$  clusters can't be distinguished.

### B. Channel Diversity of the Backscatter Tags

In our experiments, we find that the backscatter tag has the channel diversity when the excitation signal contains different frequencies. If it is able to obtain the IQ signals from different channels, there will be an opportunity for reliably distinguishing each combined state of the collided signal.

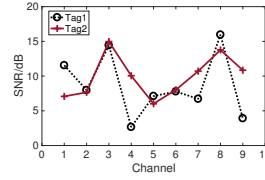


Fig. 3. The SNR of the backscatter signal at different frequencies.

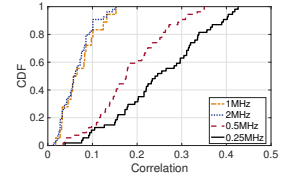


Fig. 4. The CDF of correlation between the SNR of different tags.

We first conduct experiments to observe the tag's channel diversity. The empirical results are shown in Fig. 3. We present two tags' SNR variation with the channel frequency. It is observed that the SNR will change with the channels. Furthermore, the SNR variations between two tags are different.

We collect the SNR at all channels for the tag  $i$  as a vector  $SNR(i)$  and calculate the Pearson Correlations between the tags to observe whether these tags have a similar frequency responses. The Pearson Correlation is calculated as:

$$\rho(X, Y) = \frac{E[(X - E(X))(Y - E(Y))]}{\sigma_x \sigma_y} \quad (1)$$

where  $\sigma_x$  and  $\sigma_y$  are the variations of  $X$  and  $Y$ . Fig. 4 shows the CDF of the correlation for 10 tags. We select the channels with 4 intervals: 250KHz, 500KHz, 1MHz, 2MHz and plot the CDFs for each interval. It is observed that the SNRs for different tags have low correlation because the correlation falls into the left part in the CDF ( $\leq 0.5$ ) and when the frequency difference between adjacent channels is larger, the correlation will approach 0. Therefore, the multiple channels with a interval of 1MHz or 2MHz will be better for concurrency decoding, since the combination of the tags signal is expected to be more different with large frequency difference.

It is worth noting that the variation patterns of the tags with the frequency of the channels are different. For example, Tag A has a higher SNR over Tag B at frequency  $f_1$ , while at frequency  $f_2$ , Tag B may have a higher SNR. It is beneficial for parallel decoding since the received signals of multiple tags will present the diversity at different channels and the undetectable state at one channel could be obvious at another channel. The frequency difference and the inter-tag difference can guarantee the opportunity for concurrently decoding tags' data.

The state-of-the-art works on parallel decoding of the collided signals are based on the symbol clustering in the IQ plane. As stated before, the clusters will overlap with each other severely due to the exponential increase of the clusters with the number of the tags. Therefore, the state transition between the overlapped clusters can't be detected. Our observation shows that even if the state transition is undetectable at one channel, it can be detected between two separable clusters at other channels. Fig. 5 shows an example with two channels. We make three tags to transmit concurrently with same data twice and each time we use a different channel to receive all the collided signals. In order to present the IQ symbol changes at the two channels clearly, we manually detect the

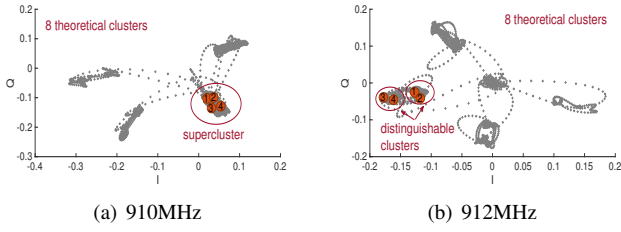


Fig. 5. The IQ symbol clusters at different channels

first IQ samples of the collided signals at two channels and synchronize the collided signals at two channels in the time domain.

We select 4 consecutive IQ symbols denoted with orange circles at two channels synchronously. The numbers in the circles denote the time sequence of the IQ symbol. We can find the 4 symbols are classified into a same cluster at the channel of 910MHz while at the channel of 912MHz, they are separated into two distinct clusters. It is clear that even though the symbols stay together in one cluster at 910MHz, there exists the state change among the 4 symbols because of the IQ information from 912MHz. The frequency difference can actually lead to the different composition of the overlapped clusters. So there exists the opportunity to represent all the combined states for collided signals with the clusters from different channels.

### C. Propagation Model of the Backscatter

A typical scenario of the signal propagation in the backscatter system is shown in Fig. 6. The sender Tx transmits the excitation signal with a single frequency  $f_c$  and there are two paths for the signal propagation from the sender Tx to the receiver Rx: the direct path and the path passing by the backscatter tag. The tag will encode its data by switching its chip impedance to reflect or absorb the excitation signal, resulting in the two different states in the received signal  $R(t)$ .

$$R(t) = h_d \exp(j2\pi f_c t) + h_f h_b h_t T(t) \exp(j2\pi f_c t) \quad (2)$$

$h_d$  is the channel parameter of the path from Tx to Rx,  $h_f$  and  $h_b$  are the channel parameters of the forward channel and backward channel between the reader and the tag correspondingly.  $h_t$  is the tag's effect on the signal and  $T(t)$  is the tag's backscatter signal to be modulated on the excitation signal.  $T(t)$  theoretically is a two-value function of 1 and 0 that corresponds to the reflection and the absorption of the tag.

However, the reflection and the absorption are not always perfect in practice. We present the equivalent circuit of the tag in Fig. 6. The left part represents the power source from the antenna with the complex antenna impedance  $Z_a$  and the right part is composed of two chip impedance  $Z_{c1}$ ,  $Z_{c2}$ . Then we can

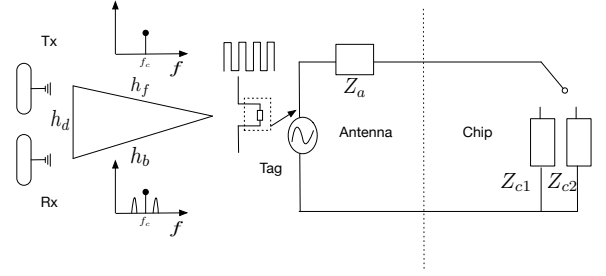


Fig. 6. A typical propagation scenario of the backscatter communication.

calculate the complex reflection coefficient of the tag in terms of these impedances as:

$$\Gamma = \frac{Z_{c1,2} - Z_a^*}{Z_{c1,2} + Z_a^*} \quad (3)$$

$Z_a^*$  is the complex conjugate of the antenna impedance  $Z_a$ . It can be observed that when the chip impedance is equal to  $Z_a^*$ , the coefficient is 0 so that the tag absorbs the signal. Otherwise if the chip impedance is  $\infty$ , the reflection coefficient will be 1, resulting in the total reflection of the signal. Actually, the chip impedance can vary with the frequency of the excitation signal and the transmitting power because the chip in the tag is a nonlinear circuit. Therefore, it is expected that the two states presented in the received signal will also change if we change the frequency of the excitation signal.

## IV. DESIGN OVERVIEW

There are two major issues should be considered in our design: 1) How to support the backscatter transmission with multiple channels; 2) How to parallel decode the collided tags' signal with IQ signals from multiple channels.

In this section, we propose Canon, a system that combines the IQ information at multiple channels to reliably decode the tags' signals concurrently. Fig. 7 presents the overview of Canon. We design the MCB module to support the generation of the excitation signal at multiple channels and the filtering of the backscatter signals at each channel. The sender will first send generated excitation signals with multiple channels and the tags switch its impedance to modulate their signals on the excitation signal. At the receiver, when receiving the signal, it first filters the backscatter signals at different channels and then separates the filtered IQ signals to different clusters. Theoretically, when there are  $N$  tags concurrently backscattering the signals,  $2^N$  clusters will be formed in the IQ plane corresponding to the  $2^N$  combined states. However, in practice, the reflection difference of the tags will cause the overlapping of the clusters so that the IQ information at a single frequency is not enough for decoding. We design the MCCU module that exploits the IQ clusters from all channels to find the correct representations of the  $2^N$  combined states and decode the data from the tags concurrently.

## V. MULTI-CARRIER BACKSCATTER

COTS readers can only transmit the excitation signal with a single frequency at one channel. How to design the reader to

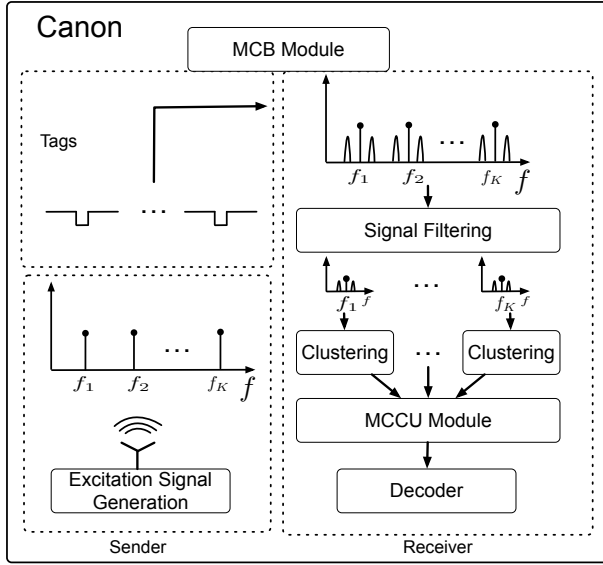


Fig. 7. The overview of Canon

support the excitation signal with multiple frequencies will be a problem. Because we want that the backscatter signals are only modulated on a single frequency carrier at each channel and the backscatter signal won't be interfered by the signals at other channels.

#### A. Generating the Excitation Signal

In Canon, we design the MCB module to realize the multi-channel excitation signal. we combine multiple single-tone signal in the baseband and then modulate the baseband signal to a carrier wave with frequency  $f_c$  to simulate a multi-channel excitation signal  $S(t)$ .

$$S(t) = (e^{j2\pi f_1 t} + e^{j2\pi f_2 t} + \dots + e^{j2\pi f_K t})e^{j2\pi f_c t} = \sum_{i=1}^K e^{j2\pi(f_i + f_c)t} \quad (4)$$

In practice, the frequency interval between  $f_i$  is set to be equal as  $\Delta f$ . According to the observation in Section III-B,  $\Delta f$  should be at least 1MHz to show the diversity and we should also guarantee it is larger than the bandwidth of the backscatter signal. Therefore the received signal  $R(t)$  at the reader will be the excitation signal multiplied by  $T(t)$ :

$$R(t) = \sum_{l=1}^M \sum_{i=1}^K \alpha_i e^{j2\pi(f_i + f_c)t + \phi_i} \times T_l(t) \quad (5)$$

$\alpha_i$  and  $\phi_i$  are the amplitude and phase introduced by the propagation path and the tag at the  $i$ -th frequency.  $M$  is the number of the tags.

In Canon, when receiving the signal, the reader will first eliminate the carrier wave with the complex signal generated locally. Since we use the same reader to transmit the excitation

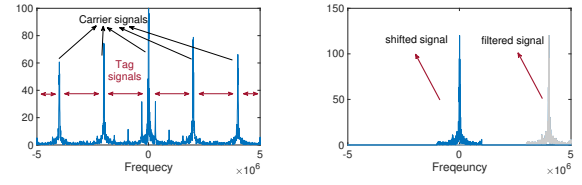


Fig. 8. The frequency domain of Fig. 9. The filtered signals at one the received signal.

signal and receive the signal so there is no frequency offset between the clocks at the sender and the receiver.

$$R(t) = \sum_{l=1}^M \sum_{i=1}^K \alpha_i e^{j2\pi(f_i + f_c)t + \phi_i} \times T_l(t) \times e^{-j2\pi f_c t} = \sum_{l=1}^M \sum_{i=1}^K \alpha_i e^{j2\pi f_i t + \phi_i} \times T_l(t) \quad (6)$$

Since the signal will be sampled discretely with a sampling rate  $f_s$ , the signal will be:

$$R[n] = \sum_{l=1}^M \sum_{i=1}^K \alpha_i e^{j2\pi \frac{f_i}{f_s} n + \phi_i} \times T_l[n] \quad (7)$$

The received signal is the baseband signal entangled by the backscatter signal and it remains a problem how to extract the backscatter signal at each channel without interference. MCB considers the explicit frequency distribution of the received signal and solves the problem in the frequency domain by signal filtering.

#### B. Filtering the Backscatter Signal

The frequency domain of the received signal is shown in Fig. 8. Tag's signal  $T(t)$  is encoded with FM0 or Miller encoding schemes and has a limited bandwidth. In Fig. 8, 0, 1, 2, 3MHz are the frequencies of the excitation signals in the baseband and the symmetric frequency spectrum centered at these frequencies are the backscatter signals. The goal of the signal filtering is to extract the backscatter signals centered at each frequency.

In order to extract the IQ signal at frequency  $f_i$ , we first use FFT to obtain the frequency spectrum of the signal, then keep those frequency components corresponding to the backscatter signals carried on frequency  $f_i$  as shown in Fig. 9. The output of the IFFT on the frequency spectrum is the backscatter signal just on frequency  $f_i$ . However, directly using this signal for IQ clustering is impossible since the signal  $B[n]$  contains the carrier signal with frequency  $f_i$ :

$$B[n] = \sum_{l=1}^M \alpha_i e^{j2\pi \frac{f_i}{f_s} n + \phi_i} \times T_l[n] \quad (8)$$

The discrete sampling on the carrier signal  $e^{j2\pi \frac{f_i}{f_s} n}$  will increase the number of the IQ clusters. Suppose  $f_i = 1\text{MHz}$  and  $f_s = 5\text{MHz}$ , there could be  $2 \times f_s / f_i = 10$  clusters with just 1 tag. Therefore, we should cancel out the carrier signal



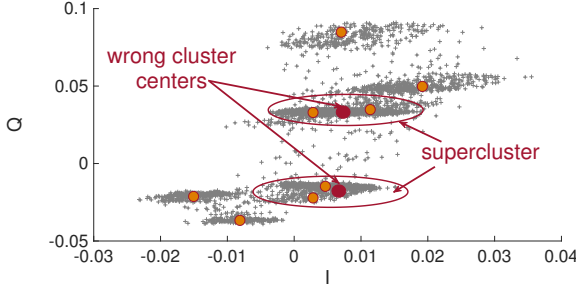


Fig. 10. The wrongly-detected clusters with the density-based algorithm.

by multiplying a complex signal with frequency  $-f_i$  and the number of the clusters will be  $2^n$  theoretically.

In practice, according to our observations in Section III-A, there are superclusters that cause the incomplete mappings from the tags' states to the clusters. In Canon, by exploiting the channel diversity among tags, we could find the correct representations of every tags' combined state for decoding.

## VI. MULTI-CHANNEL CLUSTER UNION

The critical part to use the IQ information for parallel decoding is whether we can correctly find the IQ clusters that correspond to each combined state of the collided signals. Then if we can label the cluster with the combined state, we could transform the collided signals to the combined state change and decode the information. For example, there are 4 clusters for 2 tags and they can be labeled as "HH", "HL", "LH", "LL". If the state change is "HH-HL-LH-LL", we can decode the collided tags' data by extracting each tag's state change ("H-H-L-L" for the first tag and "H-L-H-L" for the second). However, due to the superclustering, it is hard to find these clusters at a single channel. Therefore, we design the MCCU algorithm to find the representation of each combined state with IQ clusters from multiple channels. In Canon, we call these representations as Union Clusters (UCs).

### A. IQ Symbol Clustering

In order to find UCs, we should first cluster the IQ symbols at each channel. Traditional density-based clustering method used in previous works can be error-prone with the superclustering. Fig. 10 shows such scenarios because the overlapped area has the highest density and can be wrongly detected as the cluster centers.

We exploit the density-based idea but determine to use both the spatial density (local density) and the time density to separate the clusters. Because we observe that the consecutive IQ symbols likely belong to the same cluster due to the high sampling rate of the reader. We will determine the cluster centers first and then designate every symbols to its cluster.

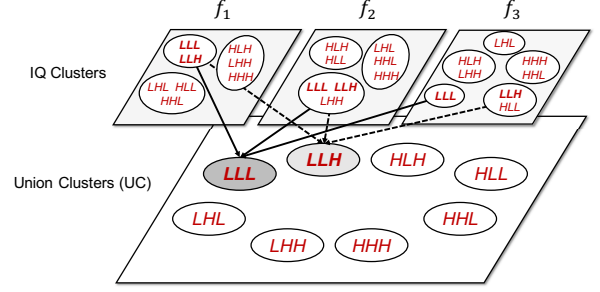


Fig. 11. An example for detecting the UC from multiple channels

*Finding the centers:* For the symbol set  $S = \{x_i\}_{i=1}^N$  and index set  $I_s = \{1, 2, \dots, N\}$ , we will define the time density of symbol  $i$  as:

$$Td(i) = \sum_{j \in W(i)} e^{-\left(\frac{d_{ij}}{d_c}\right)^2} \quad (9)$$

where  $d_{ij}$  is the distance between symbol  $x_i$  and  $x_j$  in the IQ plane,  $W(i)$  is the time window centered at symbol  $i$  and  $d_c$  is the cut-off distance. The length of the window is related to the bit duration of the tag. The spatial density is defined as:

$$Sd(i) = \sum_{j \in I_s \setminus \{i\}} e^{-\left(\frac{d_{ij}}{d_c}\right)^2} \quad (10)$$

We will find the cluster centers according to  $P_{center}(i) = Sd(i) \cdot Td(i)$ . The symbols with larger  $P_{center}$  will be more likely to be the cluster center. We will sort the  $P_{center}(i)$  in descending order and select highest  $N_{th}$  centers.  $N_{th}$  is an adaptive threshold based on the degree of the parallelism and the number of channels. We present an algorithm for adjusting the threshold in Section VII. We can now classify other symbols after the determination of the cluster centers.

*Classifying the symbols:* We will calculate the probability  $p_i^k$  that symbol  $i$  belongs to cluster  $k$  based on the distance from symbol  $i$  to the center of cluster  $k$ . We will classify the symbol  $i$  to cluster  $k$  if  $p_i^k$  is largest and  $p_i^k > P_{label}$ . Otherwise, we consider the cluster labels in the time window  $W(i)$  for symbol  $i$ . We will use the majority voting to decide the cluster label of symbol  $i$ . Then each symbol will be labeled a cluster.

### B. Finding the Union Clusters

Due to the superclustering, we can't correspond each cluster in one channel to a combined state. Therefore, we turn to use the intersection of the clusters at different channels as the UC to represent one combined state. We denote the set of combined state for  $N$  tags as  $CS = \{cs_i | i = 1, \dots, 2^N\}$  and the cluster set at the  $k$ -th channel as  $C^k = \{C_1^k, \dots, C_{N_k}^k\}$ , where  $N_k$  is the number of clusters at the  $k$ -th channel.  $C_i^k$  contains at least one combined state  $cs_i$ . For each channel  $k$ , there exist  $C_1^k \cup \dots \cup C_{N_k}^k = CS$  and  $\forall i \neq j, C_i^k \cap C_j^k = \emptyset$ .

$\forall cs_i \in CS, \exists \{q_j\}_{j=1}^k, cs_i = \bigcap_{j=1}^k C_{q_j}^j$ .  $q_j$  is the cluster index at the  $j$ -th channel. Actually, we will observe that  $cs_i$  belongs

to a cluster  $C_{q_j}^j$  at every channel. Therefore, if any two states won't keep together at a cluster for all channels, we could always find the intersections to represent each state. As shown in Fig. 11, "LLL" can be uniquely represented by the UC among three IQ clusters at the three channels although it can't be separated in each single channel.

The UCs corresponding to each combined state are uniquely determined. If two UCs share the same combination of the clusters at all channels, the IQ symbols from two states will always belong to the same clusters at all channels. The probability for such scenario can be very small because of the channel diversity.

Since UC can represent the combined state uniquely, how can we find it? We observe that the signals received at multiple channels are naturally synchronized in time domain since we receive them simultaneously in Canon. So at each sampling time, the IQ samples from all channels are from the same combined state. We only need to count the appearance of different combinations of the IQ clusters at all channels along the time to find all the UCs. In practice, due to the channel noise, we could find the wrong UCs during the transition between two combined states. In MCCU, the sampling rate of the reader is high, so the wrong UC will quickly change to the correct one. We check the time difference of the UC changes and if we find the time difference  $T_{i,i+1} < T_{edge}$ , we will mark the UC as the wrong UC.  $T_{edge}$  is set in terms of the sampling rate and the bit duration of the tag.

### C. Labeling the Union Clusters

We have found all the UCs corresponding to each combined state and now we need to match between them. As disclosed in FlipTracer [7], the probability of the transition between neighbor states is much higher. The neighbor states refer to those states with only one tag's state being different ("HHH" and "HHL" are neighbor states). If we can find all the neighbor states, we could use the existing approach [7] to decode the collided signals.

In MCCU, we first covert the sequence of the IQ signals into the sequence of the UCs and then we count all the transitions of the UCs in  $\{r_i\}$ . We build a transition matrix  $M$  and each element  $m_{i,j}$  can be calculated as the occurrence from UC  $r_i$  to UC  $r_j$   $m_{i,j} = \#(r_i \rightarrow r_j)$ . Then the transition probability between  $r_i$  and  $r_j$  will be:

$$P_{i,j} = \frac{m_{i,j} + m_{j,i}}{\sum_{k \neq i} m_{i,k} + m_{k,i}} \quad (11)$$

If we have  $N$  tags, for each UC, we will select the  $N$  UCs with the highest transition probabilities as the neighbor states. Then we can decode the collided signals in terms of the method proposed in FlipTracer.

## VII. FAULT CORRECTION

In practical, the UCs found with MCCU can be affected by the environment noise or the number of the tags. For example, the noise will cause the wrong labeling of the IQ symbols at each channel and we could find the UCs that can't correspond

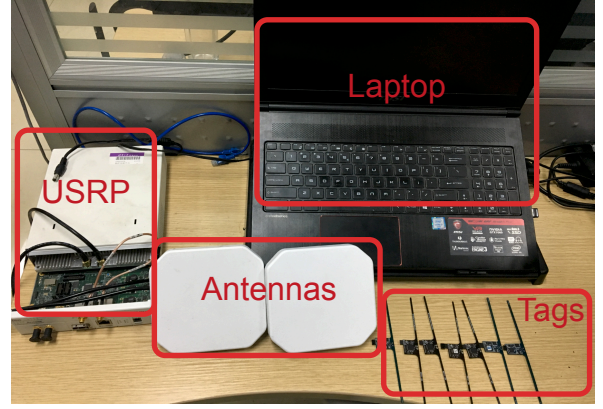


Fig. 12. The experimental setup

to any combined state. The large number of the tags will also affect the cluster labeling since there still exist the overlapping combined states that even the intersection of the clusters at all channels can't take them apart. All these situations will cause the number of UCs don't equal to  $2^N$ . In order to filter the wrong UCs and guarantee the unique representation of each combined state, we propose the methods for fault correction.

When we find all the different UC  $\{r_i\}$  with size  $N_s$ , we will count the number of the their appearance  $\#r_i$  in the collided period of  $N$  tags. If  $N_s > 2^N$ , we will sort  $\#r_i$  in descending order. For every  $r_i$ , we will also calculate the confidence of being a UC as:

$$P_{conf}(i) = \#r_i \frac{\sum P_{i,nei(i)}}{N} \quad (12)$$

where  $nei(i)$  is the  $N$  neighbors of  $r_i$ . We will select the  $2^N$  combined clusters with highest  $P_{conf}(i)$ .  $r_i$  with less appearance times and low transmission probability with its neighbors is likely caused by noise.

If  $N_s < 2^N$ , it means the clusters at the channels are not enough to represent all the combined states. In such scenarios, we will adjust the IQ symbol clustering threshold to separate more clusters at each channel. We will have an initial threshold  $N_{init} = 2^N/K$  and separate  $N_{th} = N_{init}$  clusters at each channel. If the obtained  $N_s < 2^N$ , we will select another  $(2^N - N_s)$  symbols with the highest  $P_{center}$  from all channels. So in the worst case, we still have to select  $2^N$  clusters at each channels, which is the same as the state-of-the-art approaches.

## VIII. EVALUATION

### A. Experiment Setup

We have implemented the system using the platform shown in Fig. 12. In our implementation, we use a NI USRP N210 software defined radio (SDR) as the transmitter and the receiver. The USRP is equipped with a UBX RF daughter-board and two Laird circular polarized antennas. The default sampling rate of the USRP is set to 20MHz.

The backscatter tags used in our experiments are WISP series including WISP 5.0 and WISP 4.1. In order for these tags to concurrently send their information, we modify the

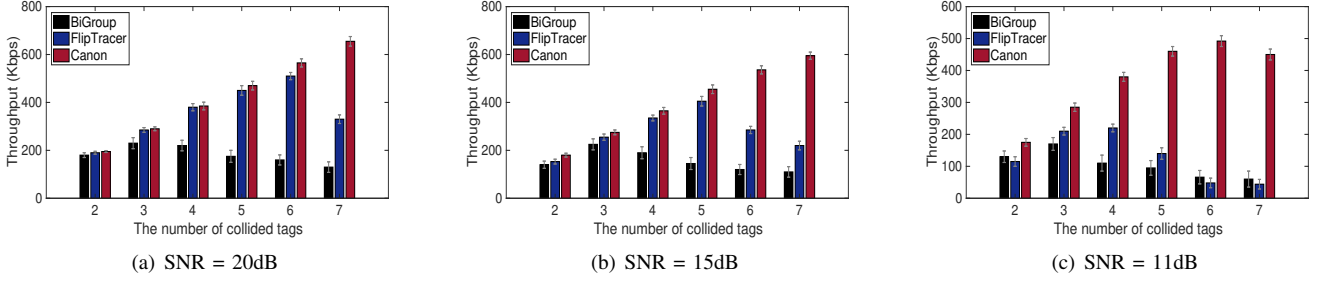


Fig. 13. The throughput of the three approaches with different number of tags and different SNRs

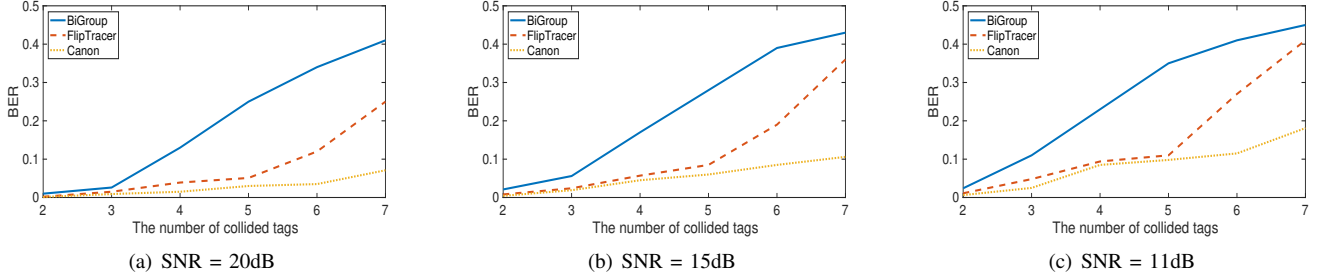


Fig. 14. The BERs of the three approaches with different number of tags and different SNRs

EPCglobal C1G2 protocol to disable the Slotted Aloha. The default backscatter bitrate is specified as 100Kbps.

### B. Methodology

In the section, we evaluate Canon in comparison with the following schemes that support the decoding of collided signals.

- **BiGroup:** This scheme assumes the different starting time and bit intervals for different tags in the collided backscatter signals. It then extracts the transition sequence of the combined states for each tag and decodes the signal with the help of the clusters in IQ domain.
- **FlipTracer:** This scheme observes the different transition probabilities between the clusters of the collided signals in IQ domain. It can identify the corresponding combined states of the clusters in IQ domain.

Canon is designed to guarantee the parallel decoding of the tags when the signals are relatively weak or there is high noise over the channels. We will consider two important metrics in our evaluation: throughput and Bit-Error-Rate (BER). We fixed the distance between the transmitting antenna and the receiving antenna. The concurrent tags are set parallel to each other and we keep the same distances between these tags to the antenna. Then we change the distance of the tags from the transmitting antenna to obtain different SNRs. We set the transmitting power of the USRP to 20dB and vary the number of concurrent tags from 2 to 7 and the default channels we used are three channels centered at 910MHz with 2MHz separation. For each settings, the concurrent tags will transmit the packet of 100 bits with FM0 encodings for 100 times and we will use the three different approaches to decode the tags' information.

### C. Overall Performance

In this section, we first evaluate the overall performance of the decoding approaches with different number of tags under different SNRs. The experimental settings are described above. The theoretical maximum throughput of the concurrent tags is the sum of the bitrate of each tag. For example, if there are 3 concurrent tags with bitrate of 100Kbps, the theoretical maximum throughput is 300Kbps.

Fig. 13 shows the throughput of all three approaches with different number of tags under different average SNRs. Fig. 13 presents the BER variation with the number of the tags under different SNRs. We can observe that when the number of the tags is 2, the throughputs of the three approaches under 3 different SNRs are all close to 200Kbps. The BERs also keep under 0.05. This is caused by the small number of combined states of the collided signal (4 states for 2 tags). The 4 clusters are easy to separate in the IQ plane so the data recovery has a higher accuracy.

However, as the number of the tags increases, the throughput of the BiGroup drops quickly and when the number is over 4, the BERs of BiGroup are higher than 0.2. The BERs of BiGroup with lower SNRs can be higher than 0.4, which means BiGroup can't work with more than 3 tags. BiGroup assumes the stable and fixed bit duration for each tag while in practice the clock of the tag is not accurate. Furthermore, the large number of the tags will make the state changes of the received signal frequent so it is easy to detect the wrong state based on the unstable bit duration.

FlipTracer has the better throughputs and the lower BERs than BiGroup. When the SNR is 20dB, the throughputs of the FlipTracer are close to the maximum throughputs with



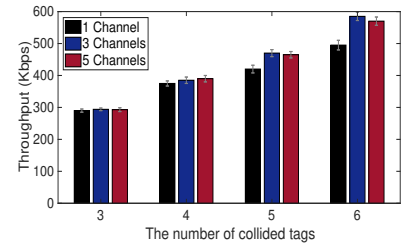
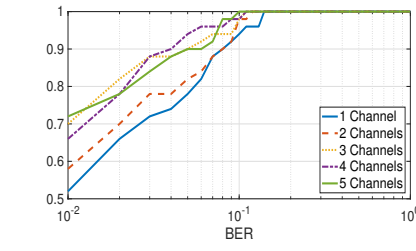
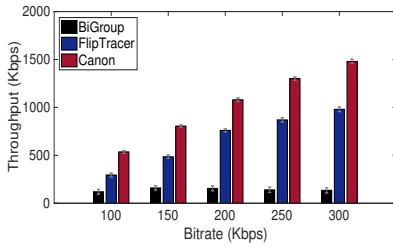


Fig. 15. The throughputs under different bitrates. Fig. 16. The CDF of the BER for 6 tags with Fig. 17. The throughputs with different number of channels.

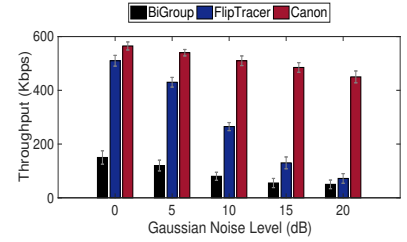
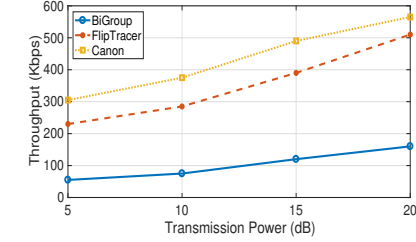
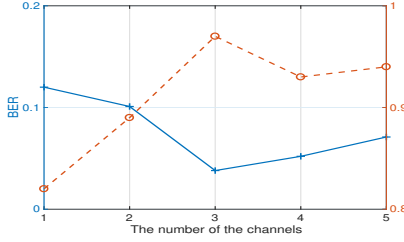


Fig. 18. The BER and PRR for 6tags with different Fig. 19. The throughputs under different trans- Fig. 20. The comparison under different channel number of channels. mission powers. conditions

less than 5 concurrent tags. The clusters in IQ plane can be correctly detected because of the high SNR. However, when there are 6 or 7 tags, there will be a sharp decrease of the throughput and the BER, since there are 64 and 128 clusters required to be separate correctly in the IQ plane. The superclustering in these IQ symbols will affect the parallel decoding. When the SNR is 15dB and 11dB, the performance of FlipTracer with 3 to 7 tags degrades correspondingly. The low SNRs of the tags will cause the severe superclustering in the IQ plane so the clustering algorithm will find the fake cluster centers. The throughput of FlipTracer with larger than 5 tags will sharply decrease because of the wrongly-detected clusters.

Canon achieves the best performance in terms of both the throughput and the BER. When the SNR is 11dB, BiGroup and FlipTracer only achieve 0.11 and 0.08 of the maximum throughput with 6 tags. Canon has the 0.82 of the maximum throughput, which is 7.5 $\times$  and 10.3 $\times$  better than BiGroup and FlipTracer respectively. Canon can also successively decode about 65% of the collided packets when 7 tags concurrently transmit. The reliability of Canon is based on the exploitation of multiple channel IQ information. BiGroup and FlipTracer have terrible performance under lower SNRs and larger number of the tags because they can't separate correctly  $2^N$  clusters in such limited IQ plane.

#### D. Impacts of Different Parameters

There are several parameters that can determine the performance of these decoding approaches such as the bitrate of each tag, the transmission power of the excitation signals and the channels used for Canon. In this section, we will evaluate Canon under different parameter.

**Bitrate:** Bitrate can affect the performance of all decoding approaches. The higher bitrate will make the state change more frequent so the 20MHz sampling rate of the USRP can't find enough samples in each IQ cluster. The current WISP tag can only support 256Kbps bitrate and we will evaluate our approach with 100, 150, 200, 250, 300Kbps bitrates. Fig. 15 shows the throughputs of 6 tags with different bitrates. The average SNR of the tags is 15dB and the transmission power is 30dBm. We can observe that in Fig. 15 Canon achieves the best throughput among the three approaches with all the bitrates. The reason is that with the redundant IQ information at three channels, Canon is more likely to separate the 64 states of the collided signal.

FlipTracer has the lower throughput than Canon because the low SNR of the tags will cause the incorrect clustering in the IQ plane. BiGroup has the lowest throughput since the high bitrate will make the signal edges stacked together. Then the unstable bit duration will misjudge the state changes for the tags. We observe that the throughput of BiGroup drops when the bitrate exceeds 200Kbps, FlipTrace and Canon also suffer the drop at the 300Kbps. At a higher bitrate, although FlipTracer and Canon can increase the robustness of the decoding, the lower SNR and close signal edges will make the clusters overlap with each other severely. However, we can still find that Canon can have a 1.6 $\times$  higher throughput than FlipTracer and a 10.8 $\times$  than BiGroup.

**Number of channels:** The number of channels can affect the performance of Canon. In this experiment, we select different number of channels centered at 910MHz and separated with 2MHz. We have selected 1-5 channels for 3-6 tags to evaluate the throughput with default 100Kbps bitrate. The results of 1, 3, 5 channels are shown in Fig. 17. We can find

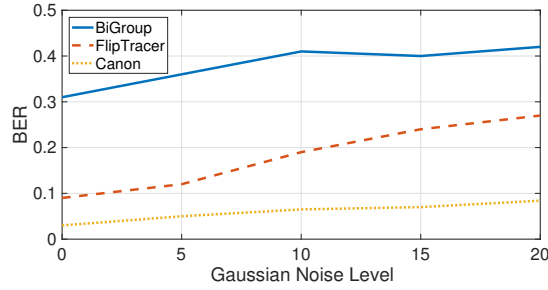


Fig. 21. The BERs with different channel conditions

that the throughput has a large increase from 1 channel to 3 channels with same number of tags. However, there is not much improvement when we increase the number of channels to 5.

This observation shows that there is a upper bound for the capacity improvement with increase of the channels and for less than 6 tags, 3 channels will be enough for both improving the throughput and saving the bandwidth. We also present the distribution of the BER with different number of channels as shown in Fig. 16. Increasing the channels to 3 can actually improve the BER because the it can distinguish the different combined states more accurately. However, with even more channels, the improvement of the BER is not obvious, because the IQ symbols from 3 channels already have the redundancy for MCCU.

We also present the BER and the Packet Reception Rate (PRR) for 6 tags with different number of channels in Fig. 18. The BER actually increases after 3 channels and the PRR decreases after 3 channels. Because the increase of the channels will also introduce the errors in labeling the IQ symbols with the clusters at each channel and it can affect the detection of the UCs. Therefore in our default settings, we select 3 channels for Canon and it works best.

**Transmission powers:** Transmission power is also a potential parameter that can affect the performance of the decoding approaches. Higher transmission power could make a larger distance between the two IQ symbol clusters of one tag in the IQ plane. We have presented the throughput of the 6 tags under different transmission powers in Fig. 19. We can observe that as the increase of the transmission power, the throughput increases. With the transmission power less than 10dB, the throughputs are lower than half of the maximum throughput while the throughput can approach the maximum throughput when the transmission power is set to 20dB. Even if Canon can utilize the multiple channel to consolidate the detection of the state change, the superclustering will be severe across all the channels with lower transmission power. In commercial RFID readers, the transmission power will be much higher than the 20dB settings in USRP. Therefore, transmission power can support the reliable decoding of Canon in practice.

**Channel Condition:** The backscatter signals are sensitive to the background noise and interference. In this section, we will evaluate the performance of Canon under different levels

of noise. In the experimental setup, we use another USRP to transmit a Gaussian noise with different transmission powers at a certain frequency 910MHz. 6 tags transmit concurrently with 100Kbps bitrate. The results are shown in Fig. 20. From the experiment, the performance of FlipTracer and BiGroup degrades with the increase of the channel noise at 910MHz while Canon almost experience no degradation with the noise at 910MHz. The throughput of Canon is  $6.25\times$  higher than FlipTracer and  $9.1\times$  higher than BiGroup. FlipTracer and BiGroup only exploit the IQ symbols at a single channel (910MHz) for clustering, which could be easily affected by the noise and interference at that channel. In Canon, the IQ symbols from multiple channels can effectively mitigate the effects of the bursty noise and interference at one channel. This can be consolidated by the BERs shown in Fig. 21. The BERs of Canon is much lower than both FlipTracer and BiGroup. Even if the noise level is 20dB, Canon can still achieve the BER less than 0.1. Canon can be more reliable and robust than state-of-the-art approaches in practice .

## IX. CONCLUSION

We have presented Canon, a reliable parallel decoding system for concurrently transmitted tags in this paper. The phenomenon of superclustering in practice can fail the parallel decoding of the multiple tags with the state-of-the-art approaches. In Canon, we observe that the channel diversity of the backscatter tag could generate different superclustering of the IQ symbols at different channels. Therefore, we design Canon to work with multi-channel excitation signals and exploit the channel diversity for reliable parallel decoding. Our experiments demonstrate that Canon can effectively improve the throughput compared with existing approaches.

## ACKNOWLEDGEMENT

This work is supported in part by National Key R&D Program of China No. 2017YFB1003000, National Natural Science Foundation of China under grant No. 61772306 and State Grid of China Research Fund.

## REFERENCES

- [1] Y. Ma, N. Selby, and F. Adib, "Drone relays for battery-free networks," in *SIGCOMM*, 2017.
- [2] L. Shanguan, Z. Li, Z. Yang, M. Li, and Y. Liu, "Otrack: Order tracking for luggage in mobile rfid systems," in *INFOCOM*, 2013.
- [3] L. Shanguan, Z. Yang, A. X. Liu, Z. Zhou, and Y. Liu, "Relative localization of rfid tags using spatial-temporal phase profiling," in *NSDI*, 2015.
- [4] J. Wang and D. Katabi, "Dude, where's my card?: Rfid positioning that works with multipath and non-line of sight," in *SIGCOMM*, 2013.
- [5] J. Wang, H. Hassanieh, D. Katabi, and P. Indyk, "Efficient and reliable low-power backscatter networks," in *SIGCOMM*, 2012.
- [6] J. Ou, M. Li, and Y. Zheng, "Come and be served: Parallel decoding for cots rfid tags," in *MobiCom*, 2015.
- [7] M. Jin, Y. He, X. Meng, Y. Zheng, D. Fang, and X. Chen, "Fliptracer: Practical parallel decoding for backscatter communication," in *MobiCom*, 2017.
- [8] P. Hu, P. Zhang, and D. Ganesan, "Leveraging interleaved signal edges for concurrent backscatter," in *HotWireless*, 2014.
- [9] —, "Laissez-faire: Fully asymmetric backscatter communication," in *SIGCOMM*, 2015.

- [10] L. Kang, K. Wu, J. Zhang, and L. M. Ni, "Ddc: A novel scheme to directly decode the collisions in uhf rfid systems," *IEEE Transactions on Parallel and Distributed Systems*, vol. 23, no. 2, pp. 263–270, 2012.
- [11] C. Mutti and C. Floerkemeier, "Cdma-based rfid systems in dense scenarios: Concepts and challenges," in *RFID*, 2008.
- [12] D. Shen, G. Woo, D. P. Reed, A. B. Lippman, and J. Wang, "Efficient and reliable low-power backscatter networks," in *RFID*, 2009.
- [13] L. Kong, L. He, Y. Gu, M.-Y. Wu, and T. He, "A parallel identification protocol for rfid systems," in *INFOCOM*, 2014.
- [14] A. N. Parks, A. Liu, S. Gollakota, and J. R. Smith, "Turbocharging ambient backscatter communication," in *SIGCOMM*, 2014.
- [15] A. Gudipati and S. Katti, "Strider: Automatic rate adaptation and collision handling," in *SIGCOMM*, 2011.
- [16] C. Angerer, R. Langwieser, and M. Rupp, "Rfid reader receivers for physical layer collision recovery," *IEEE Transactions on Communications*, vol. 58, no. 12, pp. 3526–3537, 2010.
- [17] A. Bletsas, J. Kimionis, A. G. Dimitriou, and G. N. Karystinos, "Single-antenna coherent detection of collided fm0 rfid signals," *IEEE Transactions on Communications*, vol. 60, no. 3, pp. 756–766, 2012.
- [18] R. Khasgiwale, R. Adyathaya, and D. Engels, "Extracting information from tag collisions," in *RFID*, 2009.
- [19] P. Zhang, J. Gummesson, and D. Ganesan, "Blink: A high throughput link layer for backscatter communication," in *MobiSys*, 2012.
- [20] W. Gong, H. Liu, K. Liu, Q. Ma, and Y. Liu, "Exploiting channel diversity for rate adaptation in backscatter communication networks," in *INFOCOM*, 2016.
- [21] A. L. Guillen, D. Girbau, and D. Salinas, "Radio link budgets for uhf rfid on multipath environments," *IEEE Transactions on Antennas and Propagation*, vol. 57, no. 4, pp. 1241–1251, 2009.
- [22] A. Saifullah, M. Rahman, D. Ismail, C. Lu, R. Chandra, and J. Liu, "Snow: Sensor network over white spaces," in *SenSys*, 2016.
- [23] A. Saifullah, M. Rahman, D. Ismail, C. Lu, J. Liu, and R. Chandra, "Enabling reliable, asynchronous, and bidirectional communication in sensor networks over white spaces," in *SenSys*, 2017.
- [24] H. Rahul, H. Hassanieh, and D. Katabi, "Sourcesync: A distributed wireless architecture for exploiting sender diversity," in *SIGCOMM*, 2010.